THE *IN SITU* MEASUREMENT OF LUNAR THERMAL CONDUCTIVITY

by Sydney P. Clark, Jr.

Interim Report

January 1967

Prepared under Grant No. NGR-07-004-039

Yale University

New Haven, Connecticut

The information presented herein was developed from NASA-funded work. Since the report preparation was not under NASA control, all responsibility for the material in this document must necessarily reside in the author.

NATIONAL AERONAUTICS AND SPACE ADMINISTRATION

Introduction

The measurement of heat flow at a lunar site requires knowledge of both the vertical thermal gradient and the local thermal conductivity. The former quantity can be measured more or less straight forwardly by a suitably instrumented probe emplaced in a drilled hole, but the latter presents special complications. In normal determinations of terrestrial heat flow, the conductivities of samples cored from the hole are measured in the laboratory. It is undesirable, and may even be impossible, to rely solely on this technique for lunar heat flow, since the sample may either be destroyed or may have its thermal properties seriously altered by the operations of collection and return to earth. Hence the determination of thermal conductivity *in situ* on the moon is clearly desirable and perhaps essential. This report deals with a preliminary study of a method of making this measurement which utilizes a cylindrical ring source. The results presented here form some of the fundamental criteria used in the design of a subsurface thermal probe for ALSEP by Arthur D. Little, Inc.

Theory

Consider a cylindrical hole of radius R, infinite in length, containing a cylindrical probe, also of radius R. Between $-Z$ and Z the probe consists of a heater of thermal conductivity k_1, density ρ_1, and heat capacity c_1. For $|z| > Z$ the probe has thermal properties k_2, ρ_2, and c_2, and there is no thermal resistance at $z = \pm Z$. The lunar material surrounding the hole has thermal properties k_3, ρ_3, and c_3 and there is contact resistance at $r = R$ such that a temperature drop ΔT occurs, given by $\Delta T = \frac{k_n}{H}\frac{\partial T}{\partial r}$ (the so-called radiation boundary condition). k_n would be k_1 at the outer surface of the heater, k_2 at the outer surface of the probe, and k_3 at the inner surface of the hole. The temperature is initially zero everywhere, and heat is supplied uniformly over the surface of the heater at rate Q for time $o \le t \le t_o$. We must find the temperature as a function of r, z, and t.

The conditions set forth in the preceding paragraph completely specify a boundary value problem in heat conduction, but since they involve both radial and axial flow in a heterogeneous medium, they are intractable analytically. The problem was solved by finite differences in the following way. Consider intervals in space and time δr, δz, δt, and intergers i, j, and k such that $z = j\delta z$, $t = k\delta t$, and $r = i\delta r$ for $i \le I_1$ and $r = (i - 1)\delta r$ for $i \ge I_2 = I_1 + 1$. The temperature may be regarded as a function of i, j, and k. $I_1 \delta r = I_2 \delta r = R$, the radius of the hole. However $T(I_1, j, k) \ne T(I_2, j, k)$ because of the contact resistance, although the two points are only infinitesimally separated in space. On the other hand at $z = Z = J\delta z$, the temperature is continuous. Since the temperatures are symmetric about the axis of the cylinder and also about the plane $z = o$, we need consider only positive values of r and z.

The equations used in the finite-difference calculation depend on the points at which the temperature is to be obtained. Referring to the schematic space grid shown in Figure 1, let $\alpha_1 = k_1/\rho_1 c_1$ be the thermal diffusivity in region 1, the heater, α_2 be the diffusivity in region 2, etc. Also, let $M_n^r = \alpha_n \delta t/\delta r^2$ and $M_n^z = \alpha_n \delta t/\delta z^2$, where n = 1, 2, 3. Then we have on the axis

$$T(o, j, k + 1) = T(o, j, k)\ (1 - 4M_n^r - 2M_n^z) + T(1, j, k) \cdot 4M_n^r$$
$$+ [T(o, j + 1, k) + T(o, j - 1, k)]M_n^z \quad j \ne J,\ n = 1, 2, \qquad (1)$$

$$T(o, J, k + 1) = T(o, J, k)\left[1 - \left(4\frac{\delta t}{\delta r^2} + 2\frac{\delta t}{\delta z^2}\right)\left(\frac{k_1 + k_2}{\rho_1 c_1 + \rho_2 c_2}\right)\right] + T(1, J, k) \cdot$$

$$\cdot\, 4\frac{\delta t}{\delta r^2}\,\frac{k_1 + k_2}{\rho_1 c_1 + \rho_2 c_2} + T(o, J + 1, k) \cdot 2\frac{\delta t}{\delta z^2}\,\frac{k_2}{\rho_1 c_1 + \rho_2 c_2} +$$

$$+\, T(o, J - 1, k) \cdot 2\frac{\delta t}{\delta z^2}\,\frac{k_1}{\rho_1 c_1 + \rho_2 c_2} \qquad (2)$$

In the interiors of regions 1 and 2

$$T(i, j, k + 1) = T(i, j, k)\,(1 - 2M_n^r - 2M_n^z) + [T(i, j + 1, k) + T(i, j - 1, k)]M_n^z$$

$$+ \left[\left(1 - \frac{1}{2i}\right) T(i - 1, j, k) + \left(1 + \frac{1}{2i}\right) T(i + 1, j, k)\right]M_n^r \qquad (3)$$

$$n = 1, 2,\ o < i < I_1,\ j \neq J.$$

and in region 3

$$T(i, j, k + 1) = T(i, j, k)\,(1 - 2M_3^r - 2M_3^z) + [T(i, j + 1, k) + T(i, j - 1, k)]M_3^z$$

$$+ \left[\left(1 - \frac{1}{2i-2}\right)T(i - 1, j, k) + \left(1 + \frac{1}{2i-2}\right)T(i + 1, j, k)\right]M_3^r,$$

$$i > I_2 \qquad (4)$$

Along the outer skin of the heater and probe, we have, setting $f_n = \frac{2I_1 - 1}{I_1 - 1/4} M_n^r$

$$g_n = \frac{2I_1 H\delta t}{(I_1 - 1/4)\rho_n c_n \delta r},$$

$$T(I_1, j, k + 1) = T(I_1, j, k)\,(1 - 2M_n^z - f_n - g_n)$$

$$+ [T(I_1, j - 1, k) + T(I_1, j + 1, k)]M_n^z$$

$$+ T(I_1 - 1, j, k)f_n + T(I_1 + 1, j, k)g_n,\ n = 1, 2,\ j \neq J \qquad (5)$$

and

$$T(I_1, J, k+1) = T(I_1, J, k)\Big(1 - \frac{2(K_1 + K_2)\delta t}{(\rho_1 c_1 + \rho_2 c_2)\delta z^2} - \frac{2I_1 - 1}{I_1 - 1/4}\,\frac{K_1 + K_2}{\rho_1 c_1 + \rho_2 c_2}\,\frac{\delta t}{\delta r^2}$$

$$- \frac{4I_1 h\delta t}{(I_1 - 1/4)(\rho_1 c_1 + \rho_2 c_2)\delta r}\Big) + T(I_1, J-1, k)\,\frac{2H_1\delta t}{(\rho_1 c_1 + \rho_2 c_2)\delta z^2}$$

$$+ T(I_1, J+1, k)\,\frac{2K_2\delta t}{(\rho_1 c_1 + \rho_2 c_2)\delta z^2}$$

$$+ T(I_1 - 1, J, k)\,\frac{2I_1 - 1}{I_1 - 1/4}\,\frac{K_1 + K_2}{\rho_1 c_1 + \rho_2 c_2}\,\frac{\delta t}{\delta r^2}$$

$$+ T(I_2, J, k)\,\frac{4I_1 H\delta t}{(I_1 - 1/4)(\rho_1 c_1 + \rho_2 c_2)\delta r} \tag{6}$$

At times when the heater is on, terms accounting for its effect must be added to the right sides of (5) in region 1 and (6). We write

$$q = \frac{Q\delta t}{26.289\delta r^2\delta z J(I_1 - 1/4)}, \tag{7}$$

where the numerical factor includes the conversion from total power input, $\underline{Q}$, in watts to the units of c.g.s. and calories in which the thermal properties were expressed. Then a term $\underline{q}/\rho_1\underline{c}_1$ must be added in (5) and a term $\underline{q}/(\rho_1\underline{c}_1 + \rho_2\underline{c}_2)$ must be added in (6) to account for the heat input.

Along the wall of the hole in the lunar material we have, setting

$$\underline{f}' = \frac{2I_1 + 1}{I_1 + 1/4} M_3^r \quad \text{and} \quad g' = \frac{2I_1 H\delta t}{(I_1 + 1/4)(\rho_3 c_3 \delta r}\,,$$

$$T(I_2, j, k+1) = T(I_2, j, k)(1 - 2M_3^z - f' - g') + [T(I_2, j+1, k) +$$

$$+ T(I_2, j-1, k)]M_3^z + T(I_2 + 1, j, k)f' + T(I_1, j, k)g \quad (8)$$

Finally, along the junction between the heater and the rest of the probe

$$T(i, J, k+1) = T(i, J, k)\left[1 - \frac{2(K_1 + K_2)\delta t}{(\rho_1 c_1 + \rho_2 c_2)\delta r^2} - \frac{2(K_1 + K_2)\delta t}{(\rho_1 c_1 + \rho_2 c_2)\delta z^2}\right]$$

$$+ T(i, J+1, k)\frac{2K_2\delta t}{(\rho_1 c_1 + \rho_2 c_2)\delta z^2} + T(i, J-1, k)\frac{2K_1\delta t}{(\rho_1 c_1 + \rho_2 c_2)\delta z^2}$$

$$+ \left[T(i-1, J, k)\left(1 - \frac{1}{2i}\right) + T(i+1, J, k)\left(1 + \frac{1}{2i}\right)\right]$$

$$\frac{(K_1 + K_2)\delta t}{(\rho_1 c_1 + \rho_2 c_2)\delta r^2}, \quad o < i < I_1 \quad (9)$$

Numerical stability proved to be a serious problem. In the interiors of the three regions, the stability criterion is

$$1 - 2M_n^z - 2M_n^r > o, \quad n = 1, 2, 3. \quad (10)$$

Depending on the relative thermal properties of probe, heater, and moon, a more stringent requirement may occur along the axis $\underline{i} = o$, since here the criterion is

$$1 - 2M_n^z - 4M_n^r > o, \; n = 1, 2 \quad (11)$$

But even with (10) and (11) satisfied, instability, which always originated at $\underline{i} = \underline{I}_1$ and $\underline{I}_2$, was sometimes encountered, particularly for relatively large values of $\underline{H}$. Imposing the additional constraints that

$$1 - 2M_n^z - f_n - g_n > o, \quad n = 1, 2$$

and

$$1 - 2M_3^2 - f' - g' > o,$$

did not remove the difficulty. This instability may result from the fact that the space step $\delta \underline{r}$ is effectively halved at $\underline{i} = \underline{I}_1$ and $\underline{I}_2$, but the matter remains unresolved. The time step, $\delta \underline{t}$, was simply reduced until the calculation became stable.

A second form of numerical difficulty, which may be termed semistability, was also encountered occasionally. Immediately after the heater was turned on or off, thus disturbing the system, the calculations oscillated, sometimes rather violently. The oscillations were damped, however, and the results gradually returned to a smooth trend with further cycles of iteration. This semistability could also be eliminated by reducing $\delta \underline{t}$, thus approximating more closely a smooth input of heat.

Models

A number of models of probes and of the lunar material have been subjected to numerical analysis. The results are extensive and only the more relevant ones have been selected for inclusion here. Thermal properties of 3 of the probes are shown in Table 1. The thermal conductivity of Probe 1 is too low to be practical from an engineering standpoint, but the lunar probe is expected to have properties in the range of Probes 5 and 6. Further calculations will be necessary when the final configuration of the lunar probe is established and its properties are measured.

Table 1. Thermal characteristics of probes.

No.	0	1	5	6
Heater				
k, cal/cm sec°C	0	3×10^{-7}	10^{-4}	10^{-3}
ρ, gm/cm^3	–	4×10^{-2}	0.5	0.5
c, cal/gm°C	–	0.2	0.2	0.2
Probe body				
k, cal/cm sec°C	0	3×10^{-7}	10^{-4}	10^{-3}
ρ, gm/cm^3	–	4×10^{-2}	0.5	0.5
c, cal/gm°C	–	0.2	0.2	0.2

Moon models are shown in Table 2. Three different thermal conductivities differing by factors of 10 were used, and for the lower conductivities, densities, and hence diffusivities, differing by a factor of 4 were considered. These models cover the range of values considered likely for material close to the lunar surface. The ability of a probe to discriminate between them is then a measure of its suitability.

Table 2. Thermal models of moon.

No.	k, cal/cm sec°C	ρ, gm/cm^3	c, cal/gm°C
1	10^{-5}	0.5	0.2
2	10^{-5}	2.0	0.2
6	10^{-3}	1.6	0.2
7	10^{-4}	0.5	0.2
8	10^{-4}	2.0	0.2

Another parameter entering the calculations is the contact resistance, measured by the quantity _H_. For purely radiative contact $H = 5.5 \times 10^{-12}\underline{ET}^3$, where E is the emissivity. With blackbody conditions $\underline{H} = 4.4 \times 10^{-5}$ at 200°K which is close to the mean lunar temperature. This is about the lowest value that _H_ can attain, and it is an interesting case to consider because the probe may be designed to assure purely radiative coupling. _H_ can then be calculated with confidence, whereas it otherwise remains an unknown parameter the value of which must somehow be extracted from the temperature-time curve. The effect of varying _H_ was examined by making some runs with it set at 10 times the radiative value.

The lunar probes are to be about 1.9 cm in diameter. The quantity $\delta \underline{r}$ was taken to be 0.475 cm, which places the probe skin at $\underline{i} = 2$, and $\delta \underline{z}$ was taken equal to $\delta \underline{r}$. This is a rather coarse grid, but no refinement of it was made in these preliminary studies. The simulation of a 14-hour lunar experiment required over 30 minutes on a 7094 in unfavorable cases, and it is not worthwhile to choose smaller space steps (which requires reduction of the time step as well to maintain stability) until more than hypothetical values of the probe parameters are available.

The length of the heater was taken equal to its diameter, 1.9 cm. In rough design calculations it may be desirable to approximate the probe configuration using the exact solution for radial flow from a spherical heat source, and the "square" shape chosen for the heater gives the closest possible approximation to a sphere. Thus the results of this work may be compared directly with those obtained from the spherical approximation. It should be noted that in the latter approximation no account of different thermal properties between the body of the probe and the lunar material can be taken.

<u>Numerical results</u>

It is helpful at the outset to consider the solution for an infinite cylindrical source of heat in an infinite medium. In this case the temperatures depend on the thermal conductivity and thermal diffusivity of the medium, and on the contact resistance. One could hope that the dependence on diffusivity could be removed by heating until the temperatures became steady, but with this geometry there is no steady state. The temperature of the source continues to rise indefinitely. With a heater of finite length a steady state is reached; this was an initial reason to prefer the geometry adopted here to the "line source" geometry, because the possibility exists of eliminating the diffusivity as a factor upon which the temperature depends. Another attractive feature of the present configuration is its relatively low power requirement. A line source demands a certain amount of power per unit length to produce a given temperature rise. Hence a long source requires high power. In the present case, it was found that 2 milliwatts input power gave adequate temperature rises at the heater, and this value for the heat input was used in all the calculations.

The first calculations were aimed at investigating the possibility of achieving a steady state. Results are shown in Figure 2. In this figure and those following, the temperatures are those of the outer surface of the probe. In actual lunar probes the temperature sensors will be located on the axis, but the temperature difference between these 2 points is insignificant for present purposes. It is clear from the figure that for the lower values of $\underline{K}$ the steady state is not achieved after 14 hours, and several days of heating may be required to attain it if $\underline{K}$ is less than 10^{-4}. If $K = 10^{-3}$ a few hours suffice. The probe is evidently capable of discriminating between various values of $\underline{K}$, particularly if the heater is operated at low power levels for a long time. The discrimination is best at low $\underline{K}$, and heating should last for the order of a day or more for optimum results.

Similar curves for the case of 1/10 as much contact resistance are shown in Figure 3. The discrimination is somewhat better than in Figure 2, and the curves have a different shape. The sharp initial rise in temperature is much reduced. In Figure 4 the results for a probe of higher conductivity are shown; the discrimination is not as good as in Figure 2. Clearly the thermal conductivity of the probe should be kept as low as possible.

These results show that it is likely that the temperature rise recorded during the lunar experiment will depend on the 3 quantities $\underline{K}$, α, and $\underline{H}$. Some process of curve fitting must be used to determine their values. This may be unsatisfactory since many combinations of parameters may give virtually identical results. It is therefore important to try to extract more information from the experiment, and an obvious way to do this is to record the temperatures at more than one point along the probe. The temperature rise at a point on the surface of the probe 8 cm from the center of the heater is shown in Figures 5 and 6. Figure 5 is for a probe of unrealistically low $\underline{K}$, but it shows the large differences in rise time that result from the different moon models. Intuitively one would expect the curves to be highly sensitive to α and this is born out by the difference between curves 1 and 2 of Figure 6. The rise times are about the same for the cases shown there, in which the conductivity of the probe is realistic. But if the moon is a better conductor than the probe discrimination still exists at short times, although it is not well-shown on a plot to the scale of Figure 6. Since this is just the range of conductivity at which the temperatures at the center of the heater lose discrimination, complementary information can be obtained from the second sensor.

So far we have confined the discussion to times when the heater was turned on. But a number of short-term numerical experiments have been done in which the heater was turned on for only half the time. The durations of the tests were about ½ hour. The results were that the appearances of the cooling curves were virtually identical to the heating curves, but of course inverted and displaced in time. Thus there is no new information to be obtained from the cooling curves. On the other hand, following the cooling curve in effect constitutes repeating the heating experiment, but without the necessity of expending heater power. It is always desirable to repeat experiments if only to get better statistical control.

Operations on the moon

All lunar experiments must wait until drilling disturbances have died out near the hole. The thermal gradient will be determined next and then the heater will be turned on at low power (~ 2 milliwatts). The duration of the heating cycle will be determined by the conductivity encountered. The heater will then be turned off and the cooling curve followed until ambient conditions have essentially reestablished themselves. Then, especially if a high lunar thermal conductivity is indicated by this experiment, a second heating period will be initiated. The heater power will be higher (20 milliwatts or more) so that the second sensor, displaced along the probe from the heater, will record a readily measured temperature rise. By a process of curve fitting, which is not completely thought out as yet, the quantities $\underline{K}$, α, and $\underline{H}$ will be determined. The first 2 of these automatically yield a value of $\rho\underline{c}$, which can be compared with the value measured on returned material to give a rough check on the internal consistency of the results. An alternative scheme would be to assure that H is known independently e.g. by making certain of radiative coupling alone; then only K and α need be obtained from the temperature curves and the accuracy of the measurements will be increased.

Conclusions

1. It appears feasible to measure lunar thermal conductivity using a cylindrical ring source of heat.
2. It is desirable to have 2 heating cycles, the first at a power level of a few milliwatts and the second at 10 or more times that power.
3. The duration of each heating will range from a few hours to a few days, depending on the lunar conductivity. The use of 2 sensors and 2 power levels could materially reduce the amount of heating time required.
4. There is something to be said for assuring radiative coupling to the moon so that the contact resistance can be calculated with confidence. Otherwise it represents a third unknown parameter to be determined from the temperature curves. Some discrimination of lunar conductivity is lost by this procedure, but nevertheless more accurate results will probably be obtained.
5. The best way of reducing the lunar data remains to be determined.

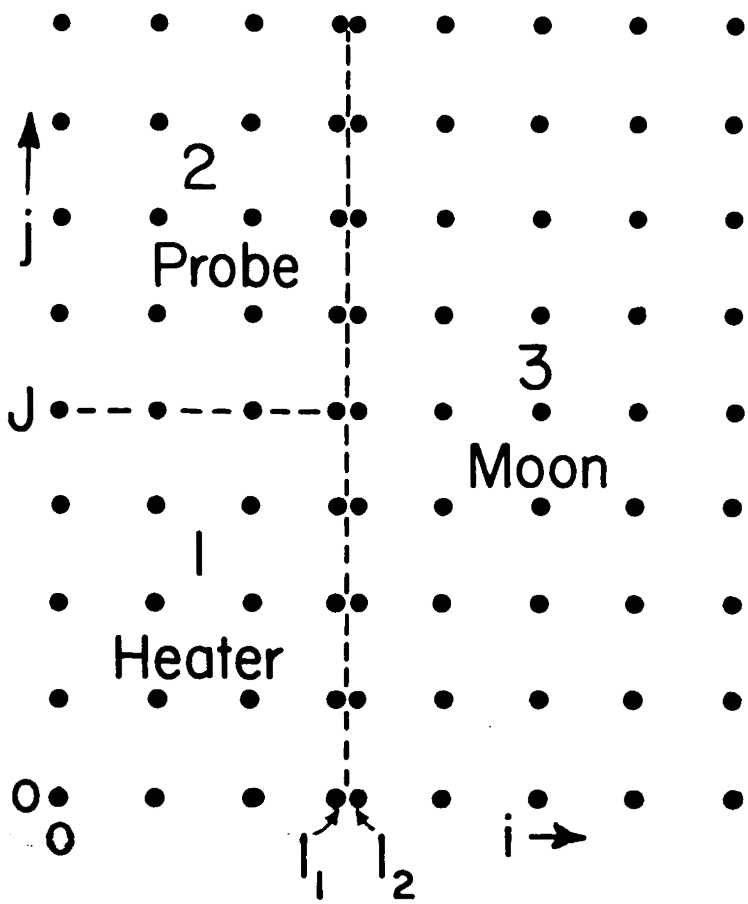

The grid used in the finite-difference approximation.

Fig. 1

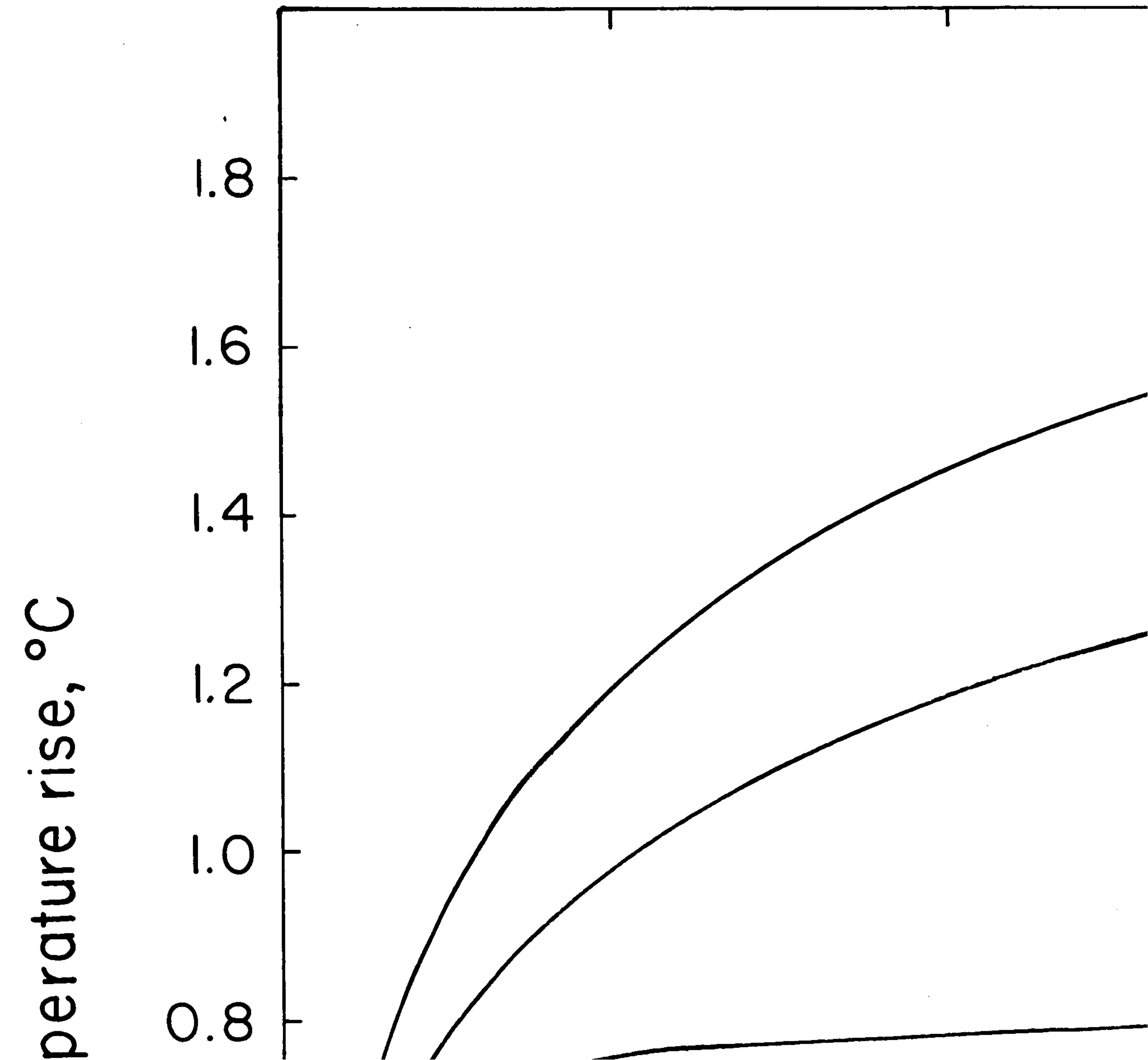
1.8
1.6
1.4
1.2
1.0
0.8
perature rise, °C

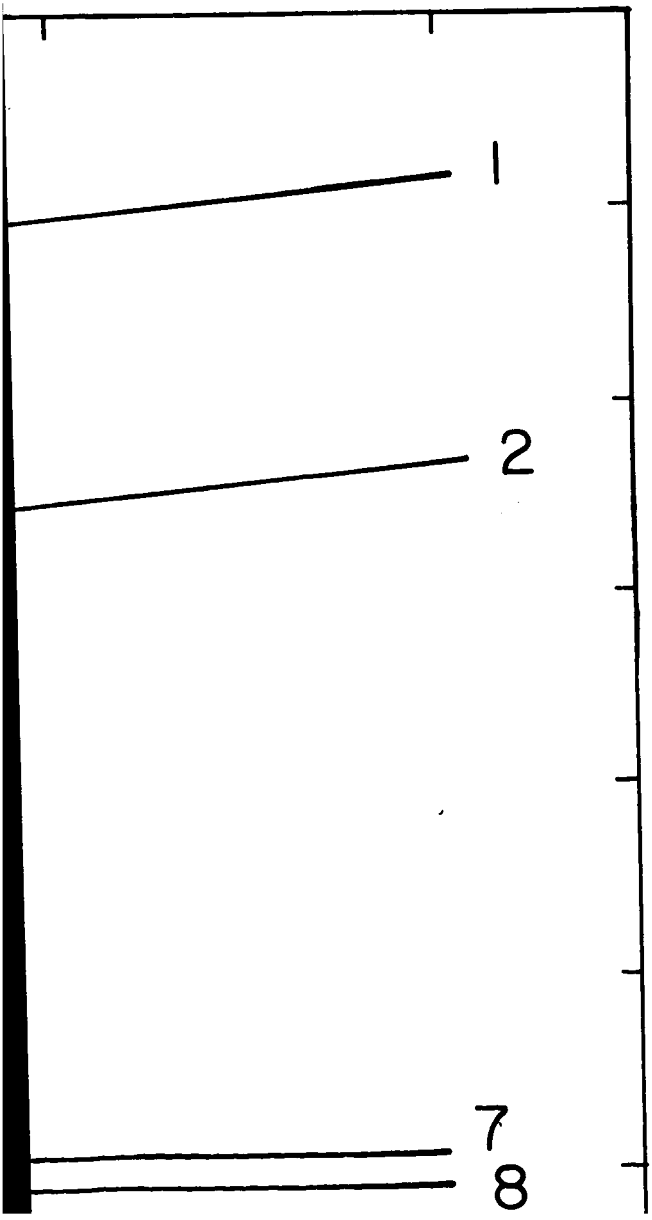
1
2
7
8

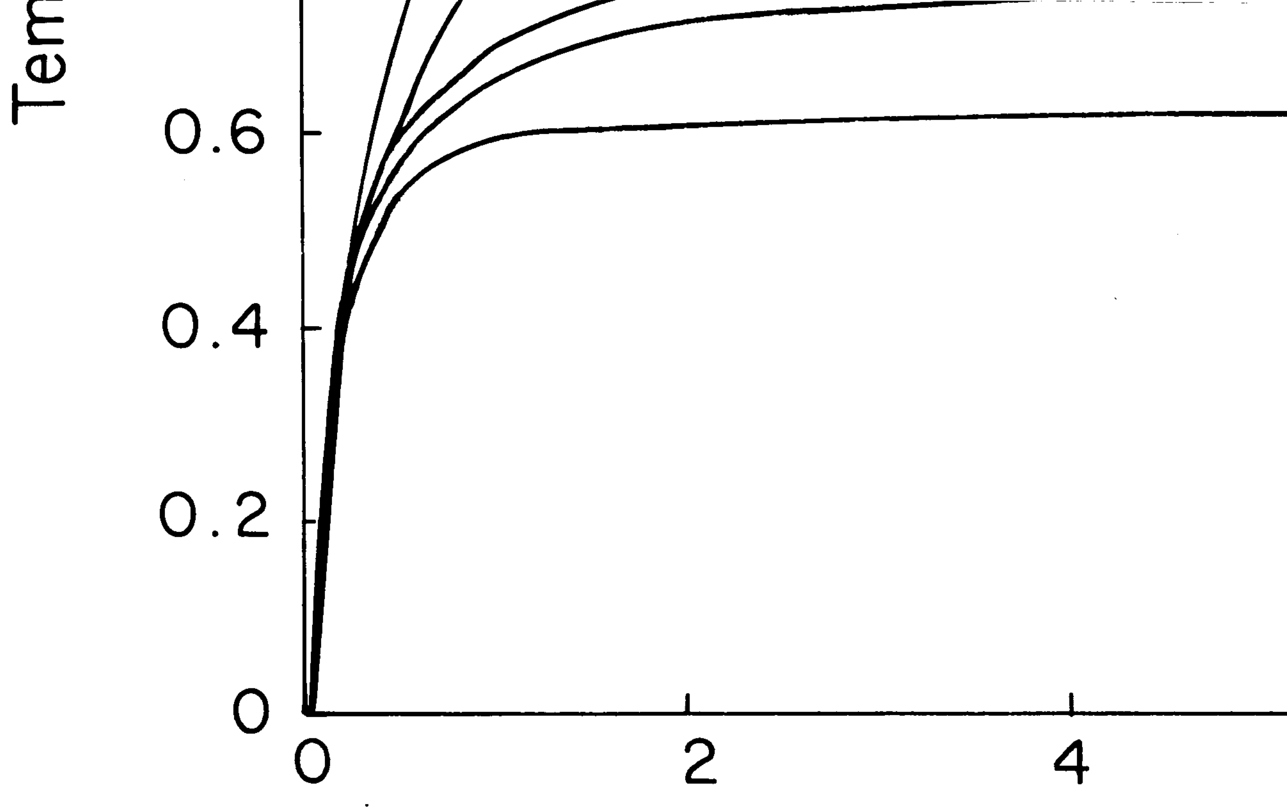

Temperature rise at the center of the heater.

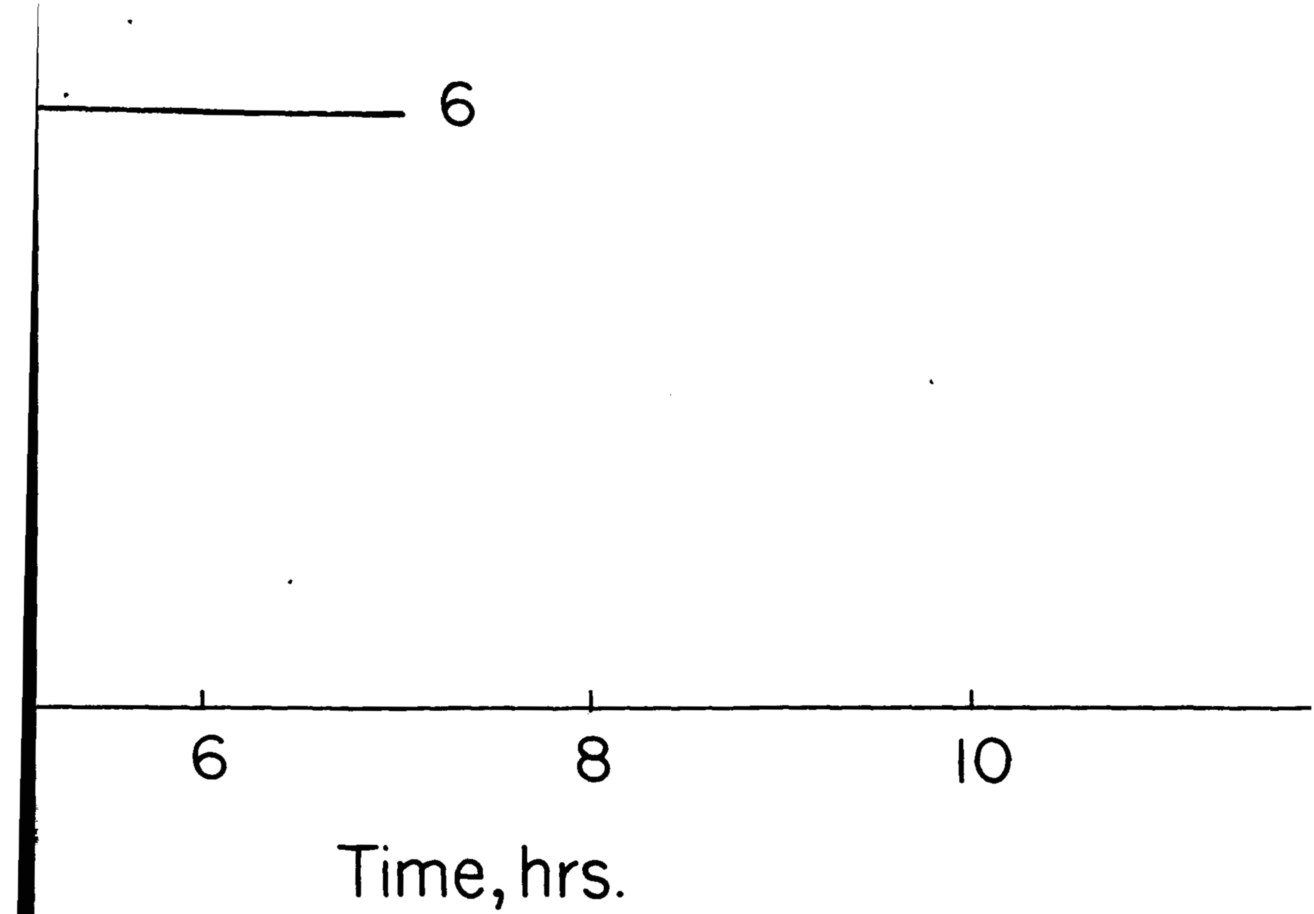

Probe 5, radiative coupling. Numbers beside the curves

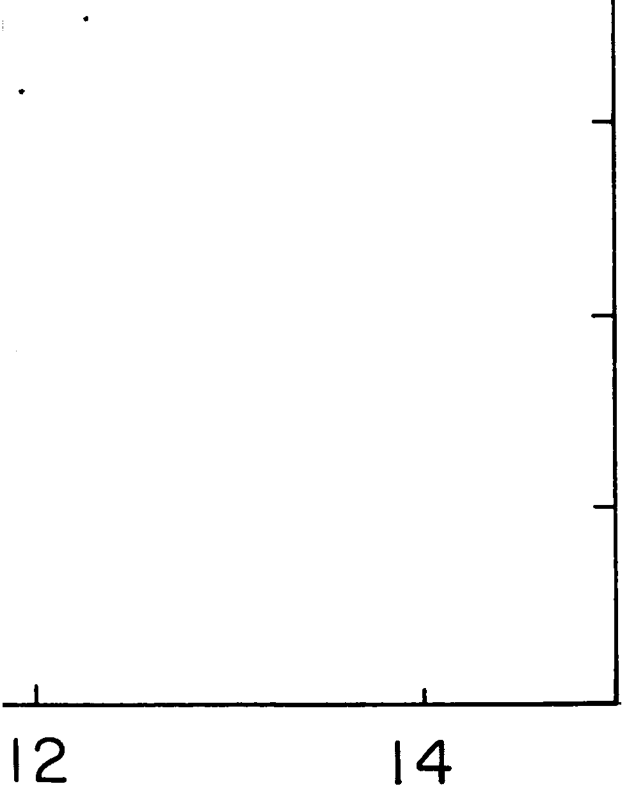

:fer to moon models (Table 2).

14-6

Fig. 2

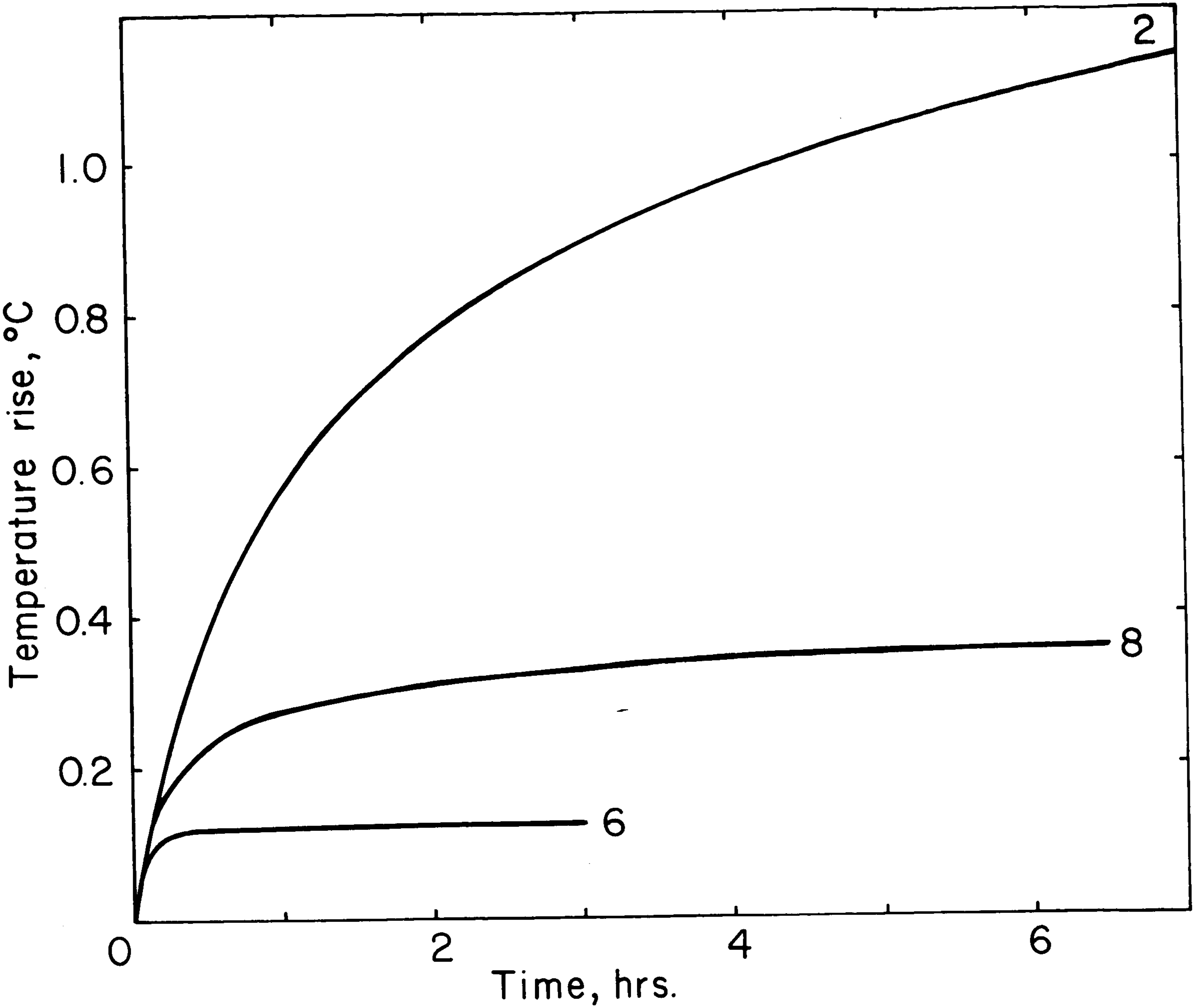

Temperature rise at the center of the heater. Probe 5, 10 times radiative coupling. Numbers beside the curves refer to moon models (Table 2).

Fig.3

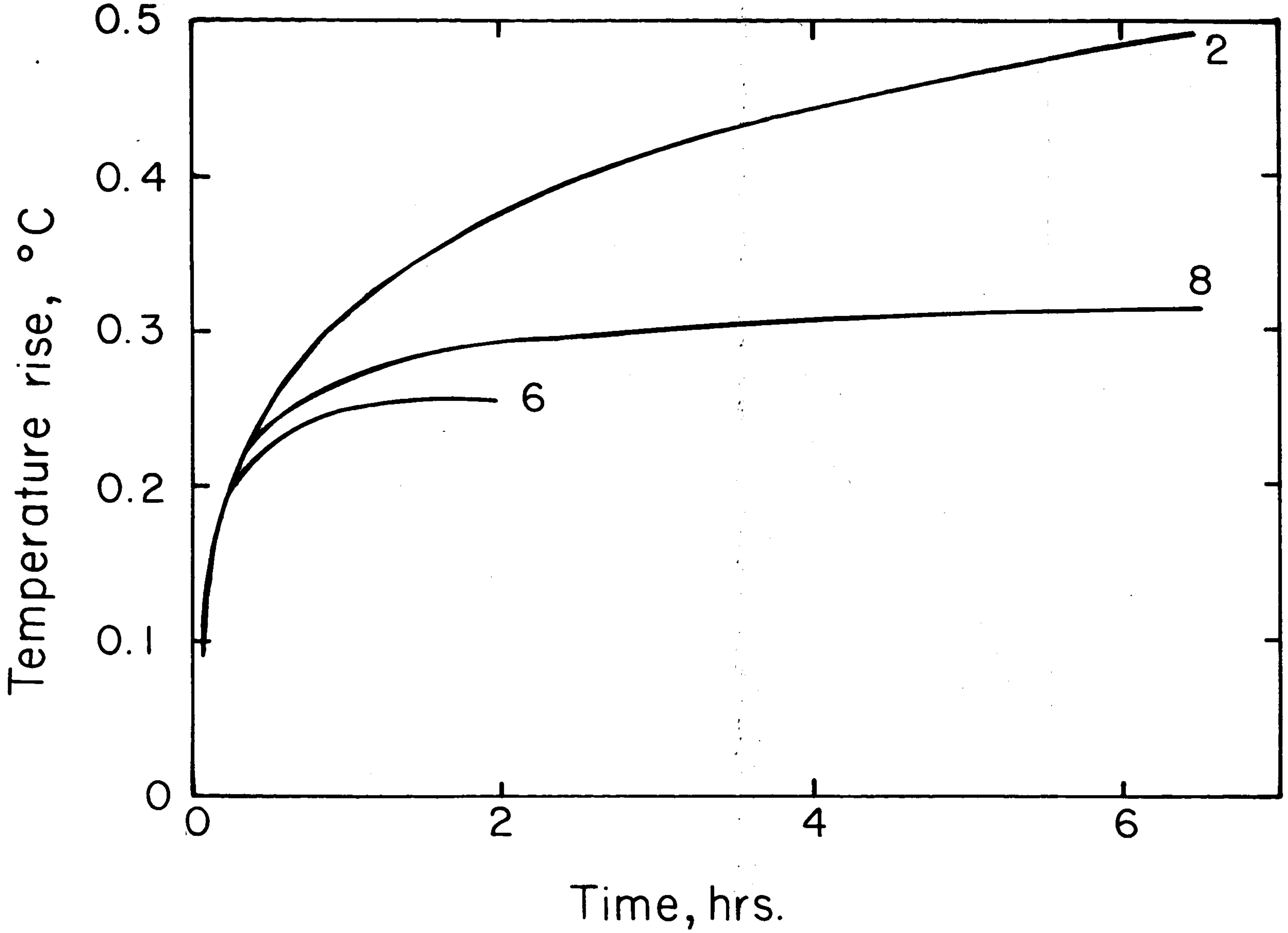

Temperature rise at the center of the heater. Probe 6, radiative coupling. Numbers beside the curves refer to moon models (Table 2).

Fig. 4

17-1

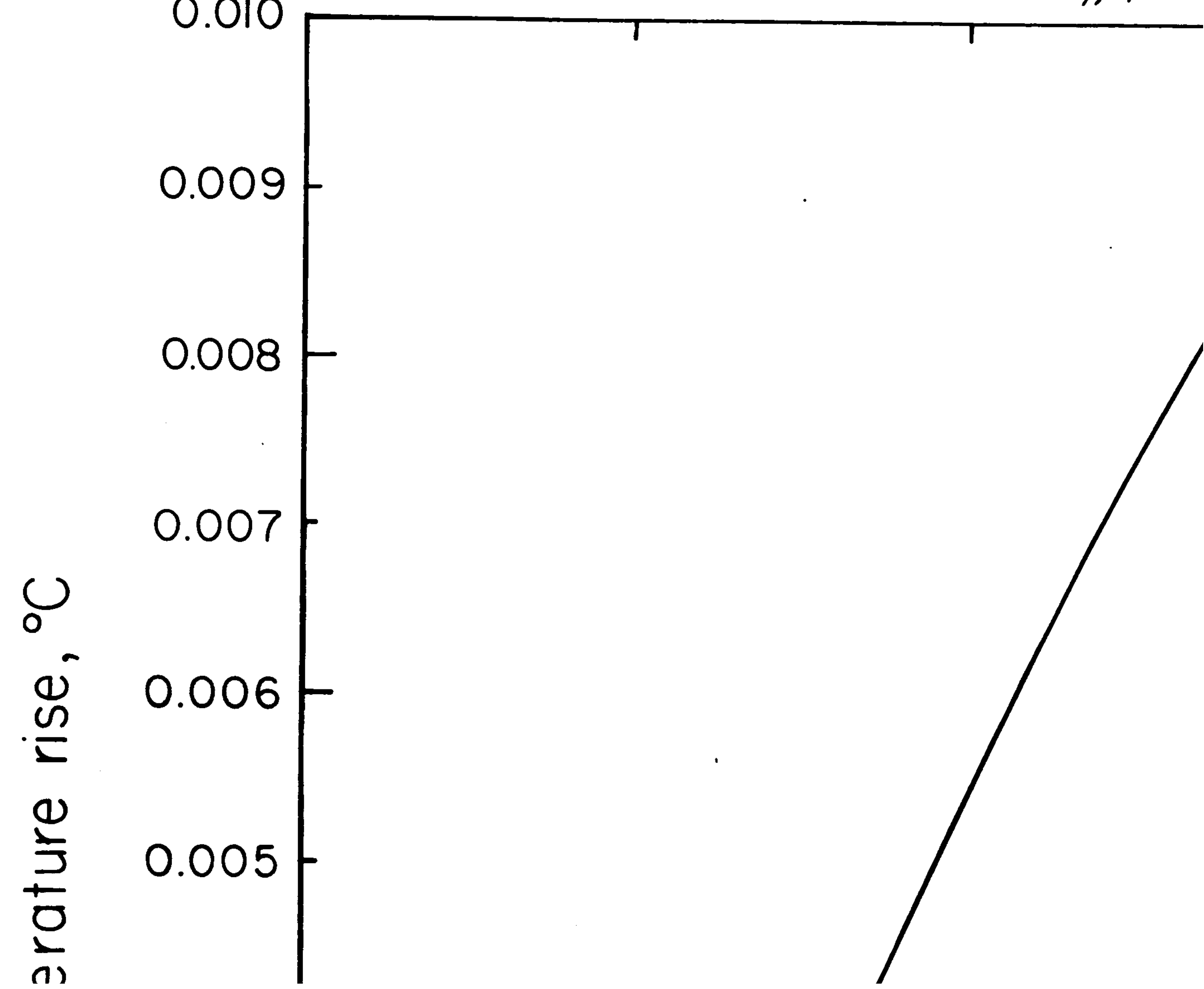

17-2

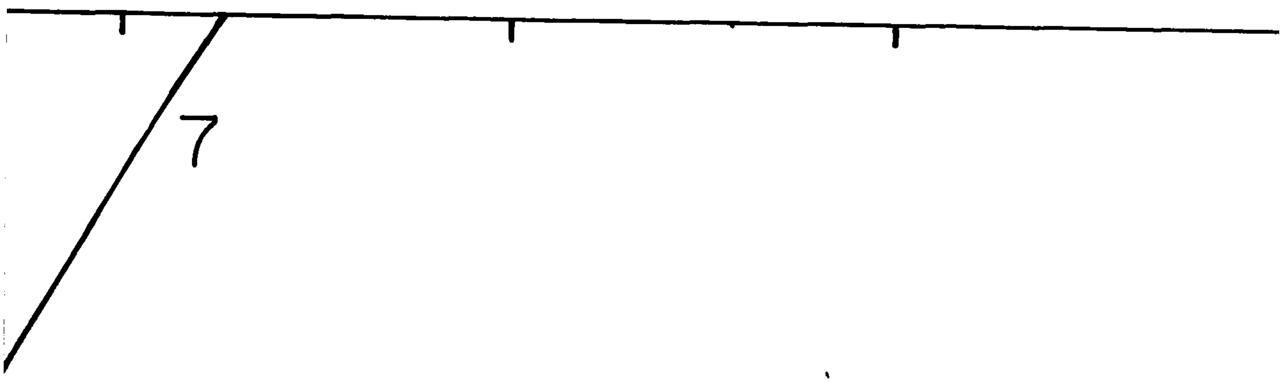

17-3

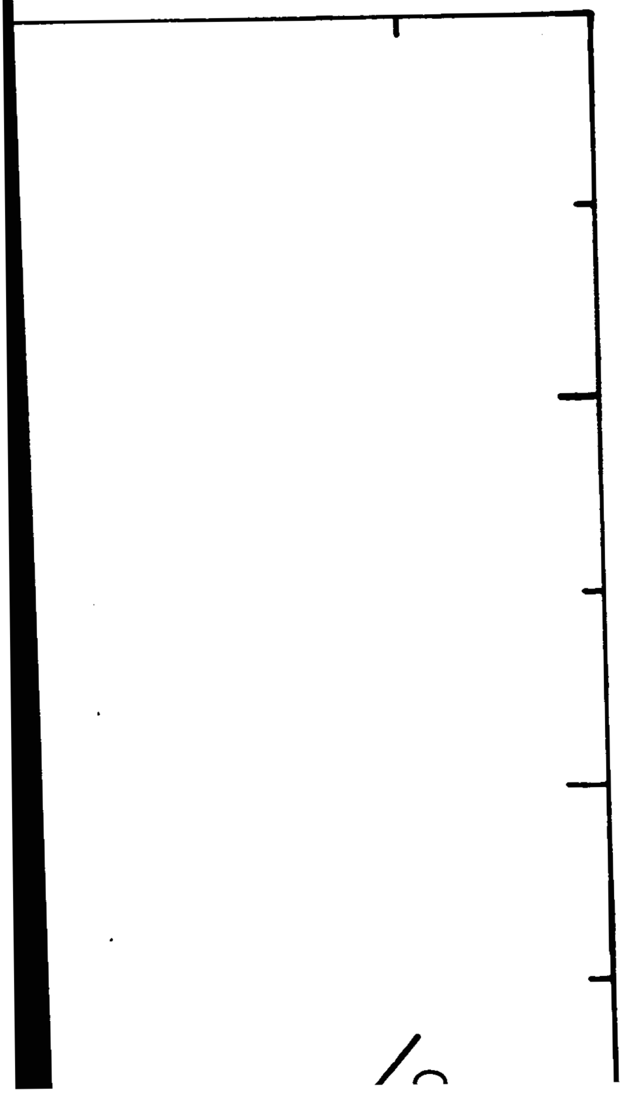

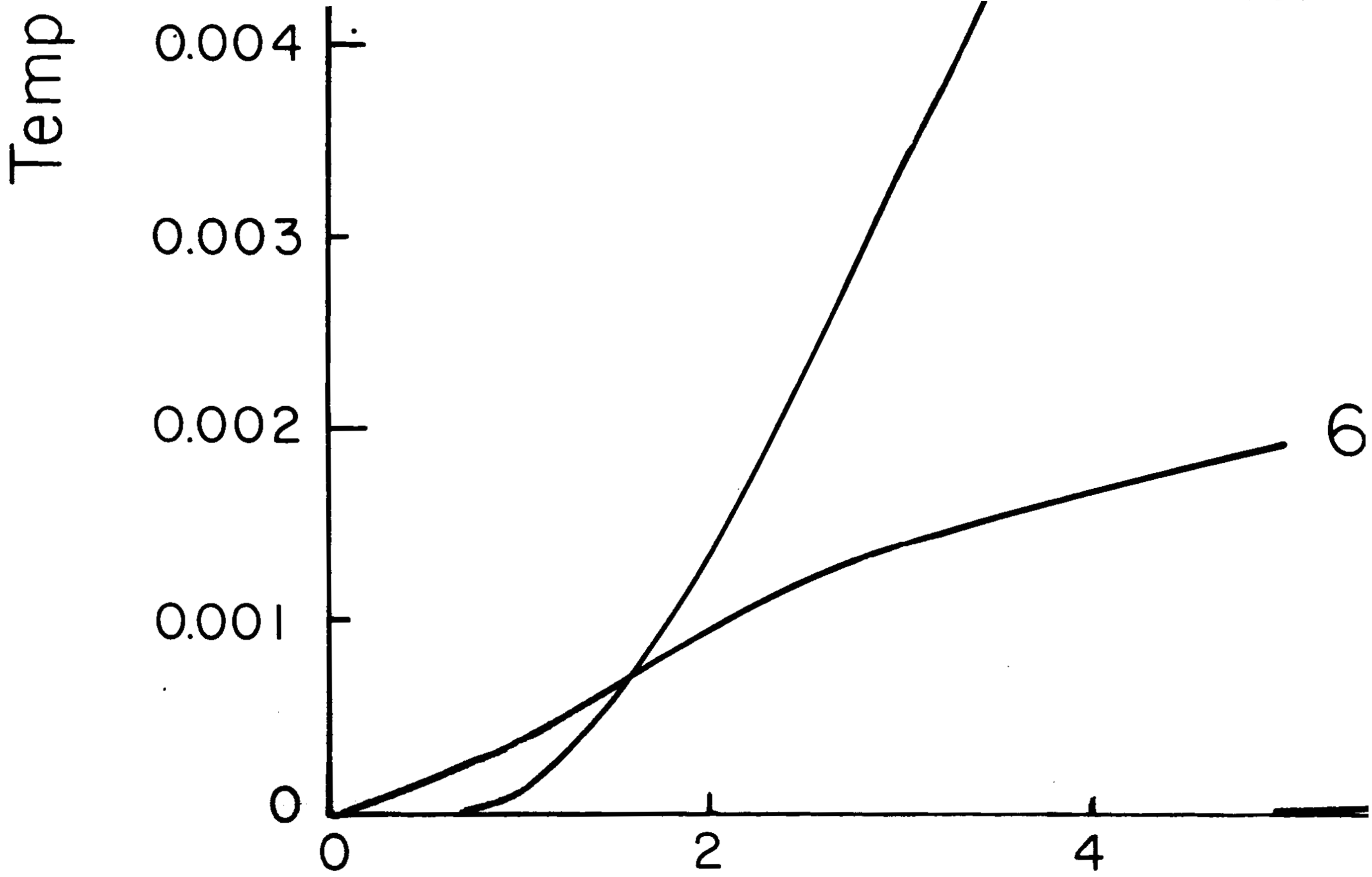

Temperature rise 8 cm from the center of the he

(Table 2).

17-4

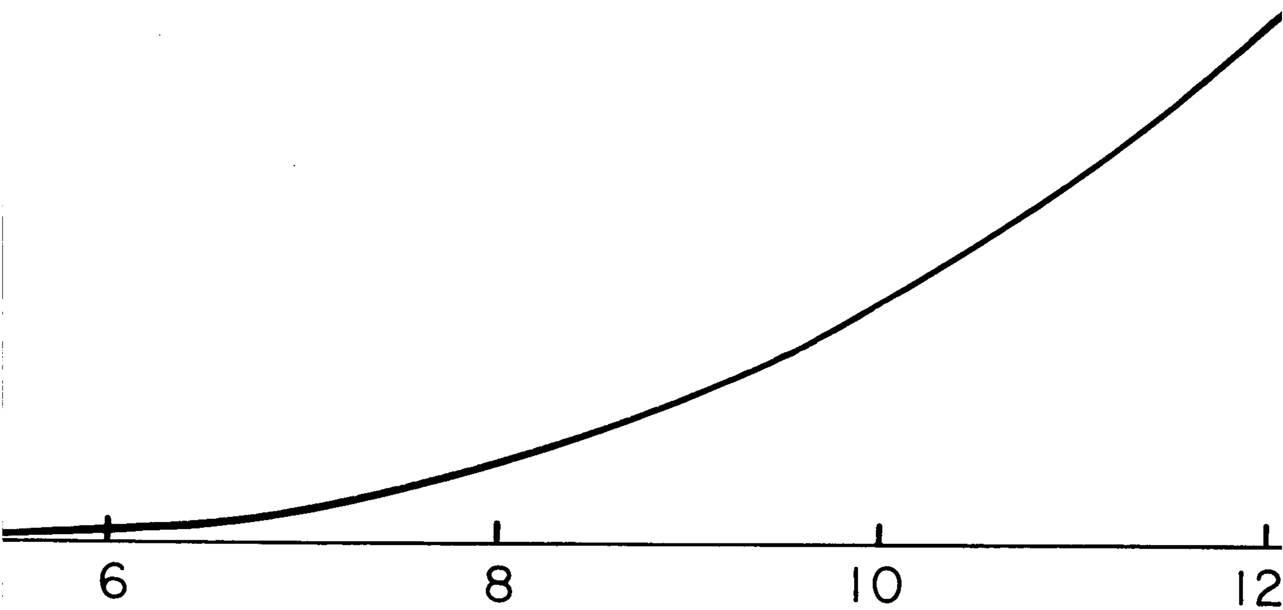

Time, hrs.

ater. Probe I, radiative coupling. Numbers beside the c

17-5

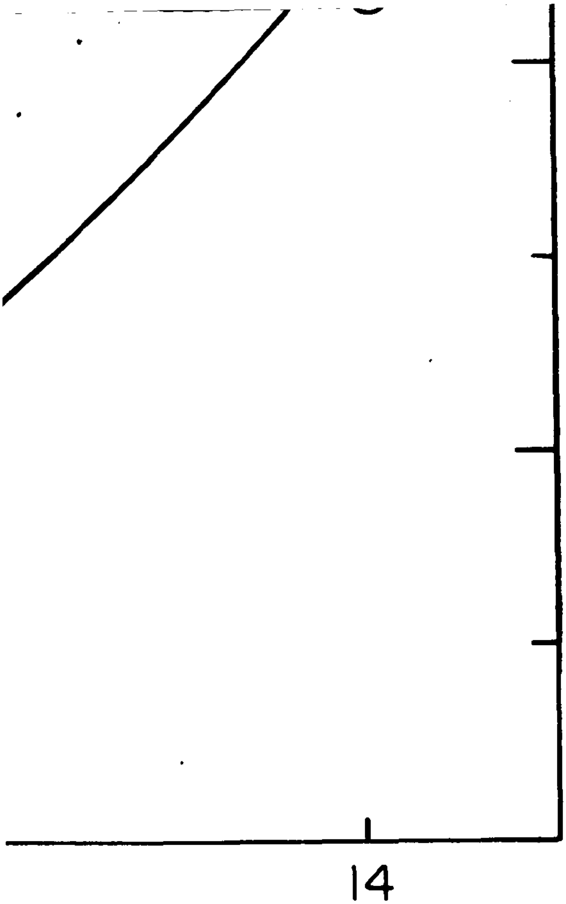

urves refer to moon models

17-6

Fig. 5

18-1

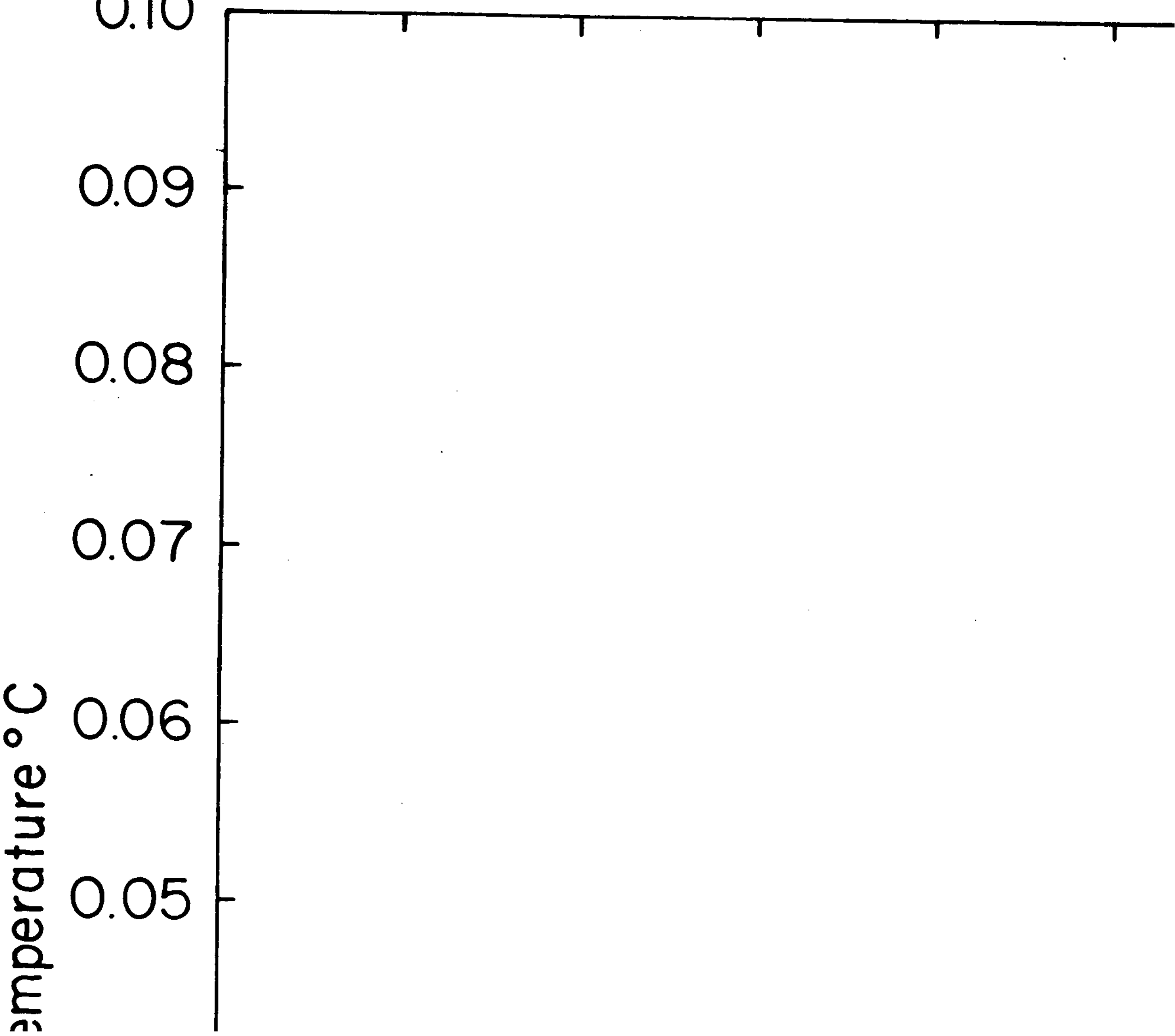

18-2

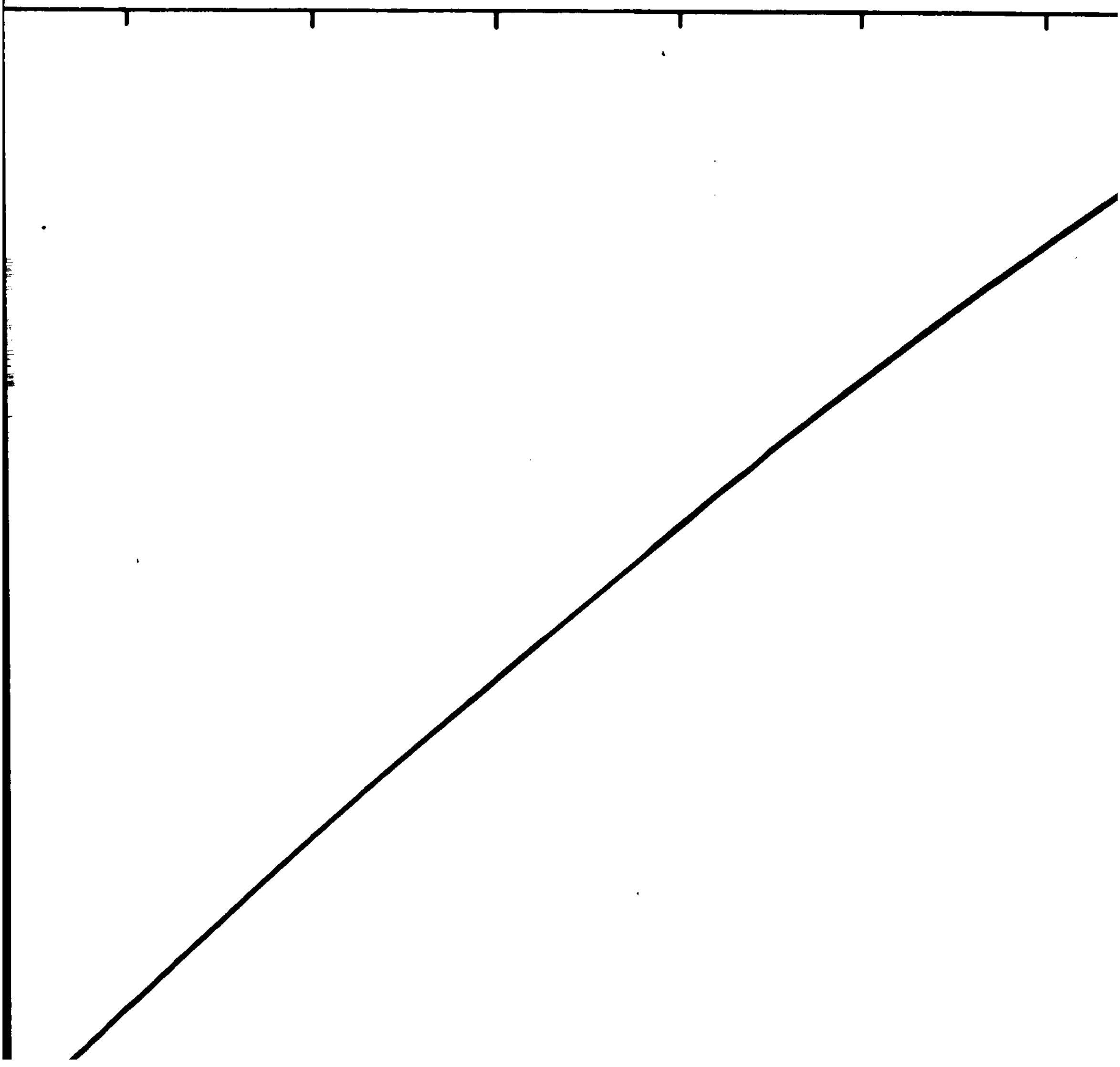

18-3

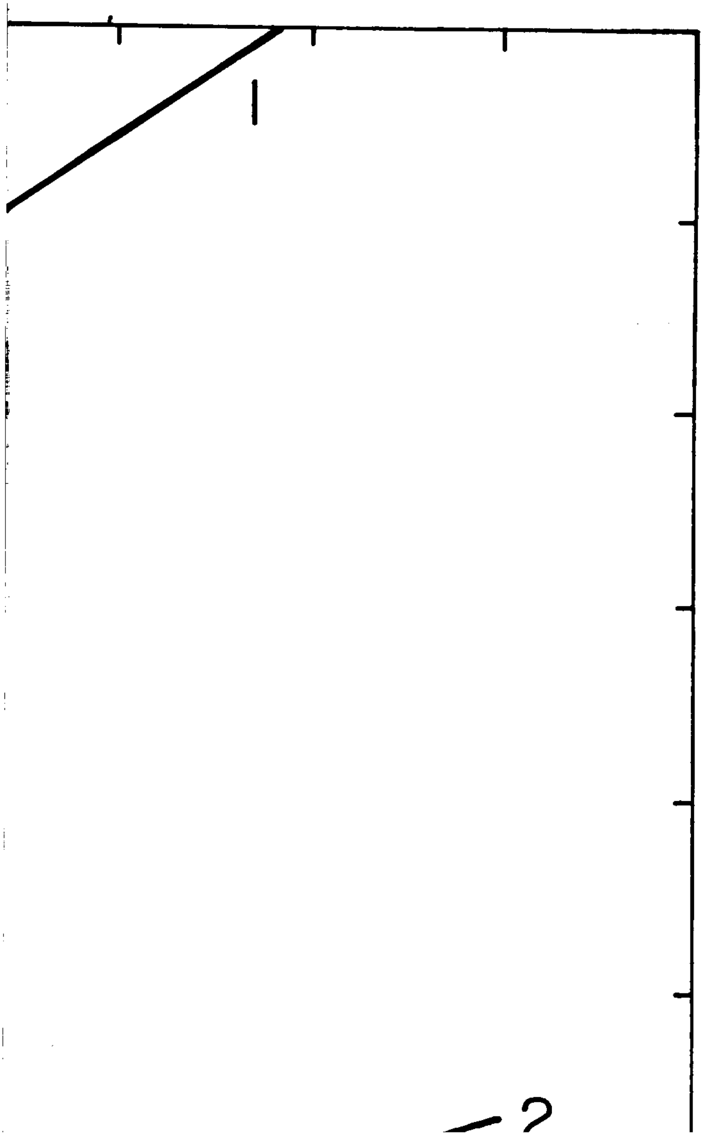

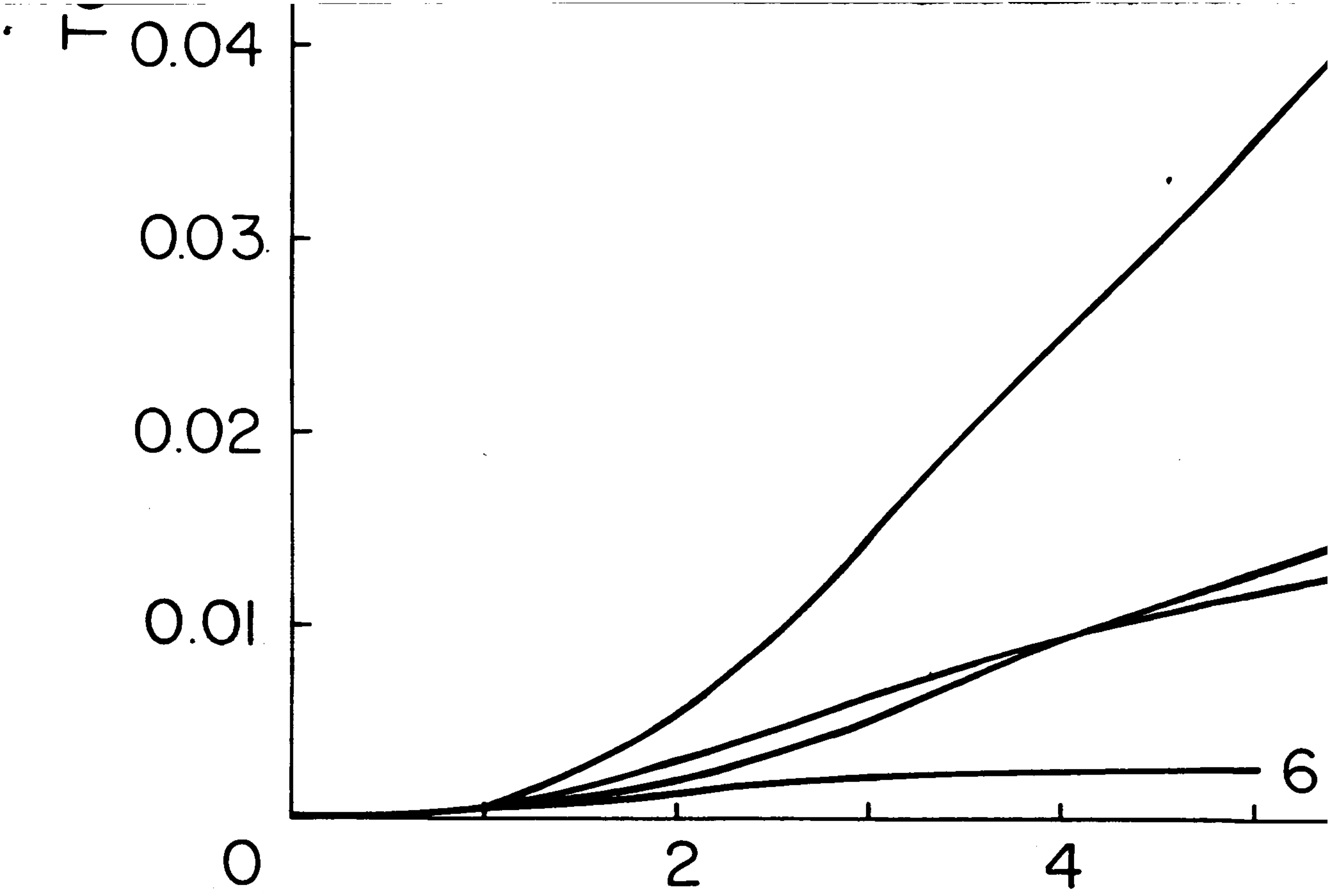

Temperature rise 8 cm from the center of the he
(Table 2)

18-4

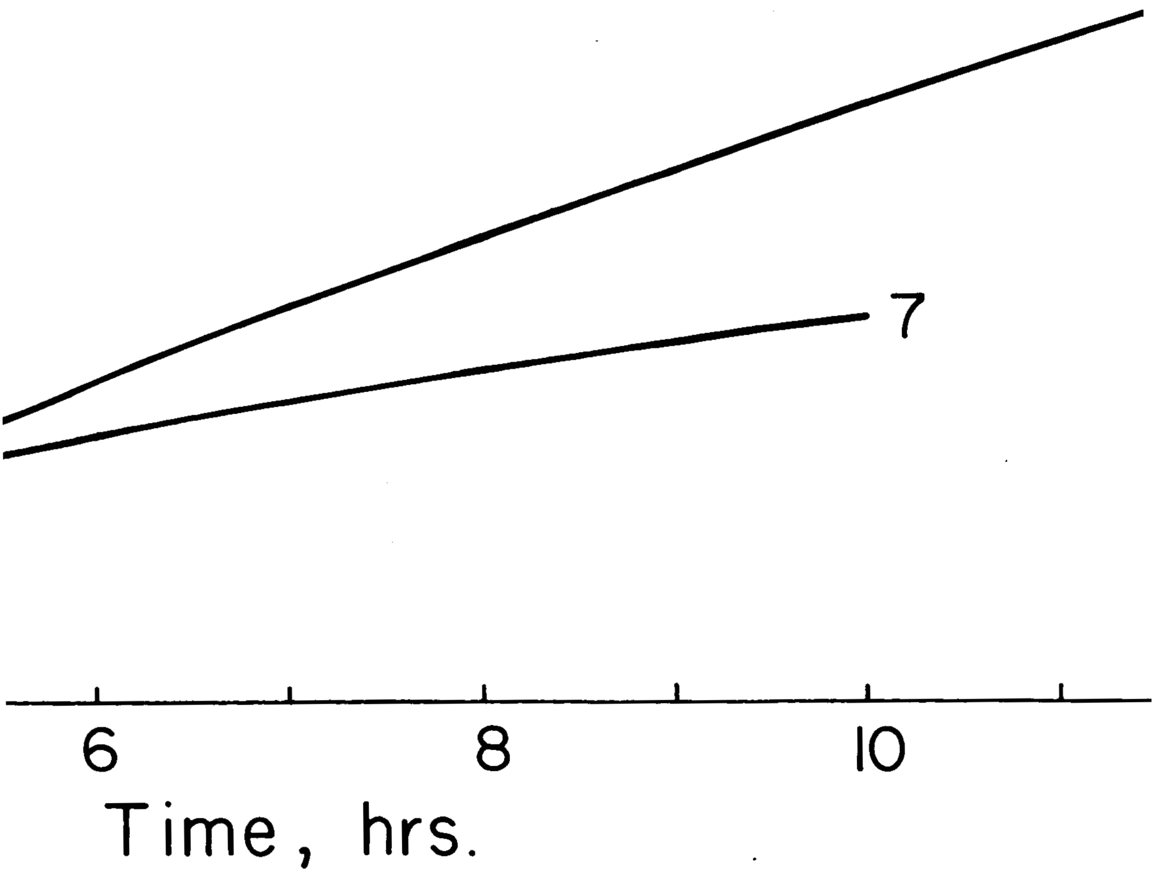

ter. Probe 5, radiative coupling. Numbers beside t

18-5

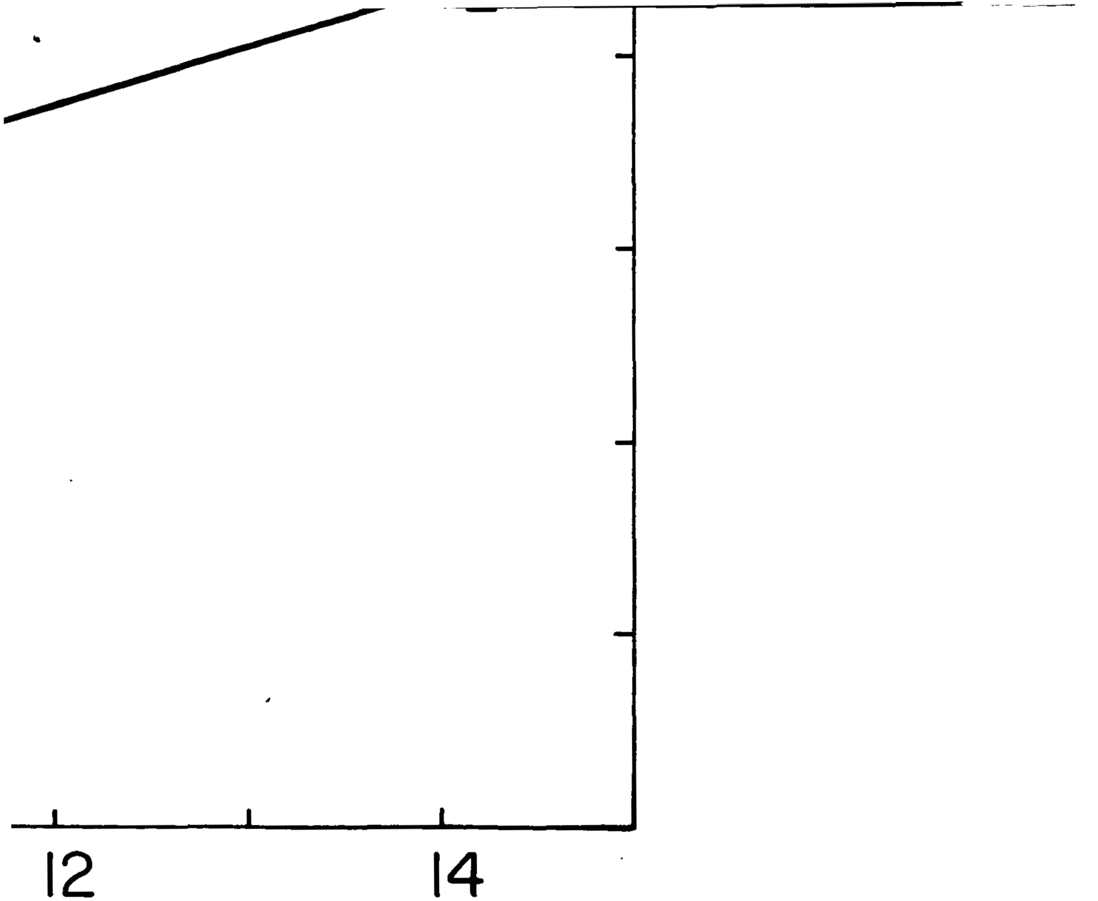

curves refer to moon models

18-6

Fig. 6